Available online at www.sciencedirect.com
ScienceDirect
Nuclear Instruments and Methods in Physics Research B 256 (2007) 187–192
NIM B
Beam Interactions with Materials & Atoms
www.elsevier.com/locate/nimb

Atomistic simulations of swift ion tracks in diamond and graphite

D. Schwen [a,b,*], E.M. Bringa [b]

[a] Institute of Physics, University of Göttingen, Tammannstr. 1, 37077 Göttingen, Germany
[b] Lawrence Livermore National Laboratory, Livermore, CA 94550, USA

Available online 20 February 2007

Abstract

We have used molecular dynamics simulations to study ion tracks in diamond and graphite. Tracks are included using a thermal spike model, i.e. a certain number of atoms within an initial track radius are given an initial excitation energy. The total energy given to the excited atoms and the length of the track determine an "effective" stopping power dE/dx. Electronic excitations in semiconductors and semimetals like diamond and graphite can diffuse far from each other or be quenched before they couple to the lattice. This effect is included by varying the number of atoms that are effectively energized within the track. We use an initial track radius of 3 nm and we find that full amorphization of this region during the first few ps only occurs when the "effective" dE/dx is larger than 6 ± 0.9 keV/nm for graphite and 10.5 ± 1.5 keV/nm for diamond. Since the "effective" dE/dx depends on the electron–phonon coupling, our simulations set bounds on the efficiency of the coupling between the electronic excitations and the lattice in this highly non-equilibrium scenario.

Keywords: Molecular dynamics; Ion tracks; Graphite; Diamond

1. Introduction

Radiation damage in both diamond and graphite has been extensively studied experimentally due to their relevance for applications in the nuclear industry and in the growing field of nanotechnology. However, MeV and GeV ion irradiation of diamond and graphite is still poorly understood. Irradiation generally produces hillocks and bumps [1,2]. There is limited or no evidence of damage tracks in diamond [2–6], which could be due to nuclear (as opposed to electronic) effects, and some evidence about damage tracks in graphite [6–8]. Experiments in amorphous carbon lead to tracks of different density and chemical character [9–11], with extremely high electronic temperatures reached in the first tens of fs of the track production [12,13]. Although these experiments probe the state of the sample at either very early times (few fs) or after microseconds/hours, there is no clear indication of the state of the material at intermediate times. Atomistic simulations offer a window for the evolution of the system at times of up to tens of ps, when most of the structural changes might take place.

There are many atomistic molecular dynamics (MD) simulations of ion and cluster bombardment of diamond and graphite at energies from eV to keV [14–22] using classical empirical potentials like the Tersoff [23], REBO potential [24], AIREBO [25] and EDIP [22] potentials and tight-binding simulations [20–22]. Previous simulations typically involve 10^3–10^5 atoms and focus on the production of point defects [14,15,17,20–22] or sputtering [16,18,19]. On the other hand, there seems to be only one attempt to model MeV–GeV bombardment: heating of small carbon volumes, surrounded by a few layers of cold material to mimic fast ion tracks, was simulated using tight binding for up to 432 atoms [26]. It was found that the sp^2/sp^3 bonds ratio depended on the track temperature and the

* Corresponding author. Address: Institute of Physics, University of Göttingen, Tammannstr. 1, 37077 Göttingen, Germany. Tel.: +49 551 397627; fax: +49 551 394493.
E-mail addresses: dschwen@gwdg.de (D. Schwen), ebringa@llnl.gov (E.M. Bringa).

0168-583X/$ - see front matter © 2006 Elsevier B.V. All rights reserved.
doi:10.1016/j.nimb.2006.12.001

relative amount of hot and cold material. In order to study the cooling of a hot track due to heat, mass, and momentum transport, much larger samples are needed. This track evolution has been studied with many semi-analytical models for tracks in semiconductors and insulators: the Coulomb explosion model [27], several flavors of the thermal spike model [28–34], etc. The thermal spike model assumes that the temperature profile in the hot track evolves according to a heat diffusion equation. This temperature history can be used to calculate defect production [28], amorphization [31–33], sputtering [29,30,33], etc. MD simulations of thermal spikes [35–40], using non-reactive pair potentials and 10^4–10^6 atoms, have shown that these semi-analytical approaches are valid only when the kinetic energy corresponding to the initial temperature of the track is much smaller than the binding energy of the material. Otherwise, there is not only heat transport, but also pressure and mass transport [35–37], and the semi-analytic assumptions break down. MD simulations comparing Coulomb explosion models to thermal spike models found no intrinsic difference between the two models [40], in the sense that a hot track will evolve in roughly the same fashion, independently of how the heat was delivered to the track atoms (by Coulomb explosion, secondary electron heating, etc.). Thanks to advances in computer power, large-scale thermal spike simulations with more than a million atoms can be now carried out in complex materials like silicates [41] and water ice [42]. Here we study thermal spikes in materials where chemistry can play a role, as described below for diamond and graphite. We first present the simulation details, then a series of results for thermal spikes at different excitation "densities", and finally discuss possible connections to experiments.

2. Simulation details

We simulate diamond and graphite using the first parametrization of the reactive bond order (REBO) potential by Brenner [24] using MDCASK [43]. This potential has a possible problem: when a melt is rapidly quenched it produces a graphitic-rich structure even at densities close to the diamond density, in disagreement with experimental results [21,22,44]. This might affect the late evolution of our track, but the influence in the amorphization threshold would be small, given that melting is reasonably described by the Brenner potential [45]. The potential by Tersoff [23] has a similar problem [21], while EDIP [21,22] and REAX potentials [46] and tight-binding simulations [15,26] produce reasonable results. Jäger and Albe increased the cut-off of the REBO potential from 0.2 to 0.225 nm to be able to produce sp^3 rich carbon in MD simulations of thin film growth [44].

Another potential problem is that even with the increased cut-off REBO has an interaction range, which, while being appropriate for diamond and for the in-plane graphite interactions, is much shorter than the separation among graphitic sheets [24]. This can be corrected by adding a van der Waals interaction using a Lennard-Jones contribution to the total energy [15,16,25]. MD simulations of radiation damage in graphite by eV–keV ion and cluster bombardment seem to indicate that the effect of the long range term in the final defect production is small [15,16] and, therefore, it has been neglected in our simulations. At small interatomic distances, the REBO potential was splined to the universal ZBL potential [47] to describe energetic collisions.

Electronic excitations in the swift ion tracks are simulated as prompt cylindrical spikes, as it has been done before for other materials using pair potentials [35–38,40–42] and embedded-atom method potentials [39]. Our simulations have sizes from $21 \times 21 \times 7$ to $43 \times 43 \times 7$ nm^3 for diamond (5.76×10^5–2.3×10^6 atoms) and $21 \times 21 \times 7$ nm^3 for graphite (3.83×10^5 atoms), and their cross section is much larger than the chosen initial track size. With these sample sizes we can include not only the hot track, but a large amount of pristine, cold material outside the track. The interface between the hot track and the "cold" sample can be tracked with time, as in the "thermal spike model" used by Toulemonde and co-workers to calculate track sizes [32,33].

We use an initial track radius within which atoms are energized by electronic excitations. This track radius, $R_{\mathrm{track}}(t=0)$, can be taken as the Bohr track radius [48], or as some function of the ion energy, velocity, etc. [32,49]. We choose an initial track radius of 3 nm, which is similar to the track radius used to study cratering and damage in hydrocarbons [50]. The radial energy distribution of the electronic system was calculated in [15,16], and most of this energy was initially contained within a radius of 3–5 nm. Recent measurements of track radii in amorphous carbon give a final track radius of less than 5 nm for bombardment with 350 MeV Au ions [11]. Since we are interested in bulk effects, periodic boundary conditions are used in all directions (we are simulating an "infinite" track). The track axis was set along the [0 0 1] direction, and in order to avoid artifacts due to size-effects, the height of the track is at least 2 times the track radius.

A fraction of atoms within $R_{\mathrm{track}}(t=0)$ are each given an excitation energy E_{exc}, which determines an "effective" stopping power $\mathrm{d}E/\mathrm{d}x$. The exact value of E_{exc} received by the atoms due to decay of the electronic excitations is not known. Ab initio tight-binding simulations of laser-induced electronic excitation in graphite and diamond have considered temperatures higher than 3 eV/atoms [51]. In addition, experimental measurements of the electronic temperature in ion-irradiated amorphous carbon using Auger electrons [12] give an upper limit to the temperature in diamond and graphite tracks. These measurements indicate temperatures of several tens of thousands of K after ~10 fs. Excitation energy was chosen to be 3 eV/atom, giving an initial temperature of ~23,000 K for the fully excited track. This energy is comparable to the one used in [26], where the upper limit studied for the track temperature was 30,000 K. A variable time step algorithm [43] is

employed in our simulations, such that time steps much smaller than 1 fs are used in the early phase of the spike, while time steps of ~1 fs can achieve energy conservation at longer times when the spike is cooler. Energy can be given to excited atoms as a delta function or as a Maxwellian distribution with mean energy E_{exc}.

These two excitation modes only differ when $E_{exc} \ll U$, [36] where U is the binding energy of the material, which is ~7 eV for diamond and graphite. Here we use a delta function distribution, since we are exploring the regime where $E_{exc} \sim U/2$ and the differences in the temperature profiles resulting from Maxwellian or delta distributions are relatively small.

We assume that all excitations decay at the same time. This approximation can be relaxed, leading only to relatively small corrections [38].

Given that diamond is a semiconductor, and that graphite is a 2D conductor (in the graphitic planes), one would expect that the initial electronic excitations will be rapidly quenched or diffuse away from each other. This means that, even if the entire volume of the track was initially excited, only a fraction of these excitations will decay close to each other and to the center of the track. Only a high concentration of excitations will lead to significant damage production [37]. Excitations decaying far from the track have small probability of producing lasting damage, since the individual excitation energy is small compared to the binding energy of the material and the displacement energy. In particular, the displacement energy in diamond is larger than 15 eV [14,15], so a single excitation of 3 eV will only lead to local heating without any defect being created in the lattice. We take into account the quenching and migration of excitations using a simple model: for the same track radius and E_{exc}/atom, we examine the role of the "efficiency" of the electron–phonon coupling by assuming different numbers of excited atoms, given as a fraction of the total number of atoms in the initial track. We consider 10, 20, 30, 40, 50, 70, 90 and 100% efficiencies. The tracks had a total of 35,587 and 23,651 atoms for diamond and graphite respectively. Therefore, these values would correspond to effective dE/dx values of 1.5, 3, 4.5, 6, 7.5, 10.5, 13.5 and 15 keV/nm in diamond; 0.9, 1.8, 2.7, 3.5, 4.4, 6.3, 8 and 8.9 keV/nm in graphite. 100% efficiency would correspond to an energy of 47/43 MeV for Au bombardment of diamond/graphite. As a summary, our model could be used to compare to ion bombardment experiments for a given ion-target pair (for a given ion mass, velocity and charge, etc.) using two free parameters: (a) the track radius; (b) the efficiency of the transfer of electronic excitations to the lattice that links the effective dE/dx with the experimental dE/dx.

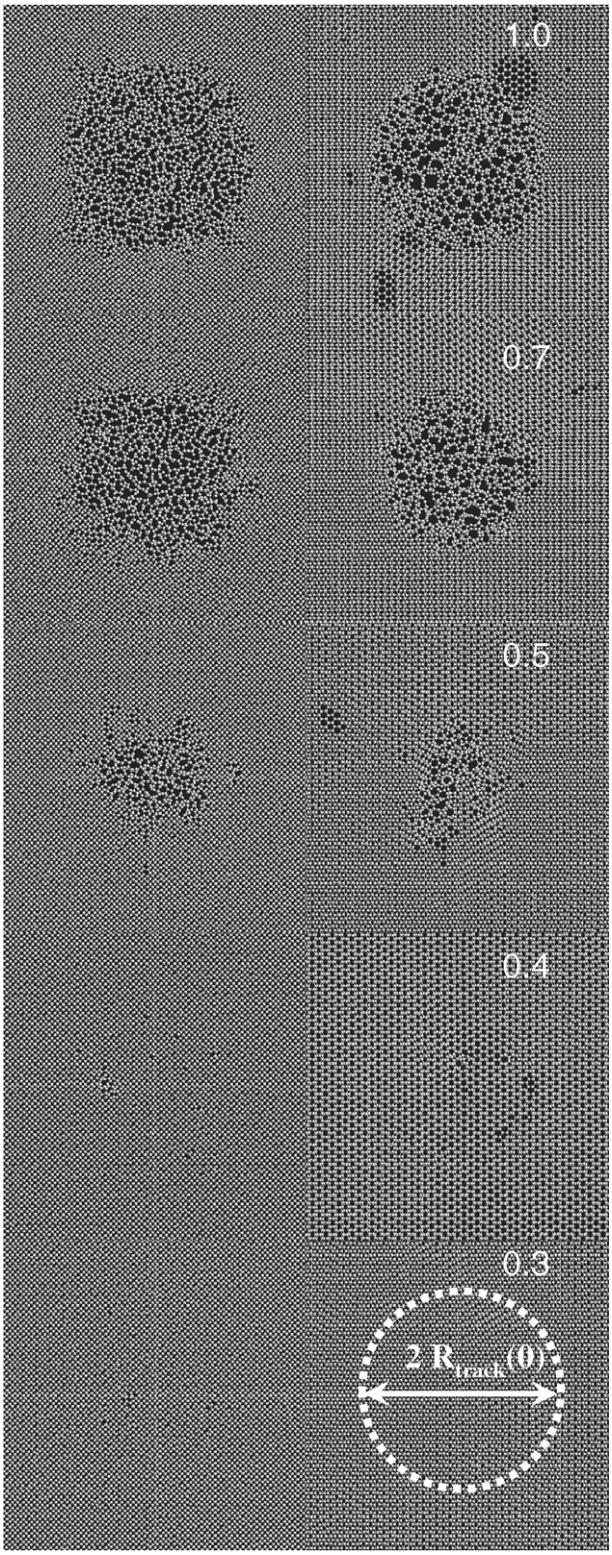

Fig. 1. Track in diamond (left column) and graphite (right column) at the end of our simulations. Efficiency (1.0 = 100%) is indicated on each row. Only a $(6\,nm)^3$ slab around the track center is shown, with the track oriented perpendicular to the plane of the figure.

3. Simulation results

Fig. 1 shows snapshots of the tracks in diamond and graphite after ~2.3 ps, for several efficiencies. As expected, point defects are created even at 30% efficiency. The crystallinity of the lattice within the original track is partially kept even at 50% excitation. Full amorphization is already observed at 70% excitation efficiency.

The large energy input that causes the defects seen in Fig. 1, will typically produce a shock wave in MD simulations of hot tracks with a large energy density [35–37]. This shock wave will transport energy and momentum away from the track, producing a cooling effect. However, due to the finite simulation size, when the wave reaches the outer boundary of the simulation box, some of the wave energy and momentum will be reflected at the boundary back towards the track. Several methods exist to decrease this reflection but are computationally expensive [52]; therefore, only a simple temperature rescaling was applied to a thin layer at the cell boundaries parallel to the track. The outgoing shock wave can be seen in the time evolution of the kinetic energy maps seen in Fig. 2 for a thin layer of the large diamond sample. There is an outgoing energy wave which follows the cubic symmetry of the diamond lattice, with [1 1 1] being the fastest direction for propagation. On the other hand, in graphite there is a roughly cylindrical wave. This is similar to the surface waves seen in graphite under cluster bombardment in [15,16]. After ~2.4 ps the peak value of the energy at the boundary is 0.05 eV. Neglecting the flow velocity correction to the temperature calculation, this energy is equivalent to a temperature of 250 K above the initial temperature of the sample. However, since this is a wave of decaying amplitude, the "temperature" of the wave when it reaches the track boundary is lower, and the increase in the track due to this spurious reflected wave is negligible compared to the track temperature. The velocity of the spike-induced wave along [1 1 1] directions is slightly supersonic according to our calculations: $v/c_0 = 1.1$, for $c_0 = 18$ km/s [53].

Because of the high radial velocities around the spike we have to remove the flow velocities from our temperature calculations.

Figs. 4 and 5 show temperature for diamond and graphite at 50% efficiency. We first show in Figs. 3(a) and 4(a) that the temperature calculated for orthogonal directions in cylindrical coordinates (radial, T_r, axial T_z and angular, T_{ang}) is roughly the same everywhere. At earlier times there are small deviations at the edge of the track, where the shock wave is being generated, and where the shock front is located, as shown for diamond by the small "bump" at $r \sim 7$–8 nm in Fig. 3(a). This indicates that, except where the temperature gradient is larger, there is local thermal quasi-equilibrium even at short times. Figs. 3(b) and 4(b) show the temperature profiles at different times. These profiles support the scenario of melting-induced amorphization at high excitation densities only. We note that the temperature at the center of the track is above melting for ~1–2 ps for graphite–diamond and 50% efficiency, and for 2–3 ps for graphite–diamond and 70% efficiency. At the end of our simulations the track temperature is well below melting. This time evolution contrasts with the

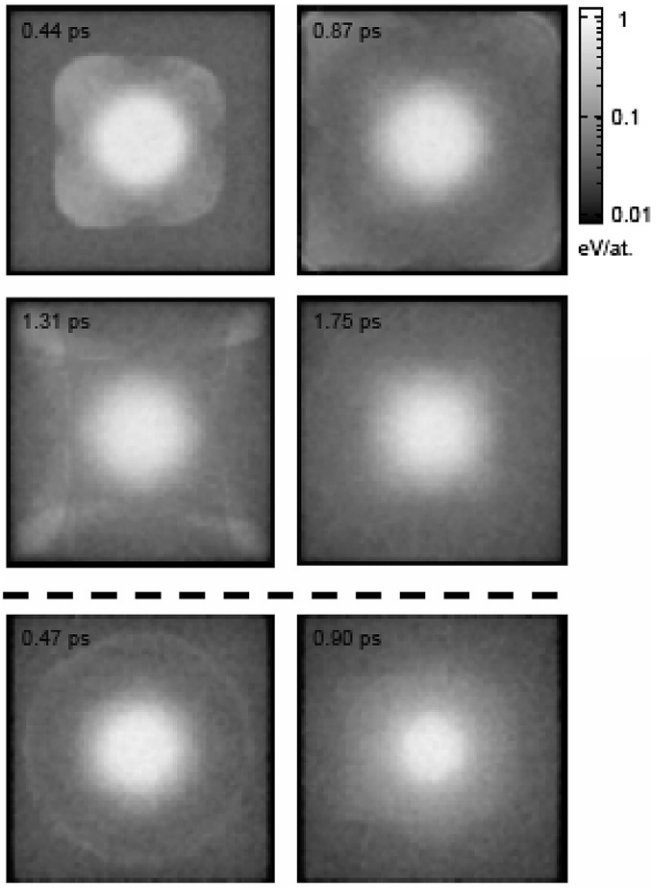

Fig. 2. Ion track in diamond, 50% efficiency (large sample). Kinetic energy maps are shown at different times. Only a slab around the track is shown, with the track oriented perpendicular to the plane of the figure.

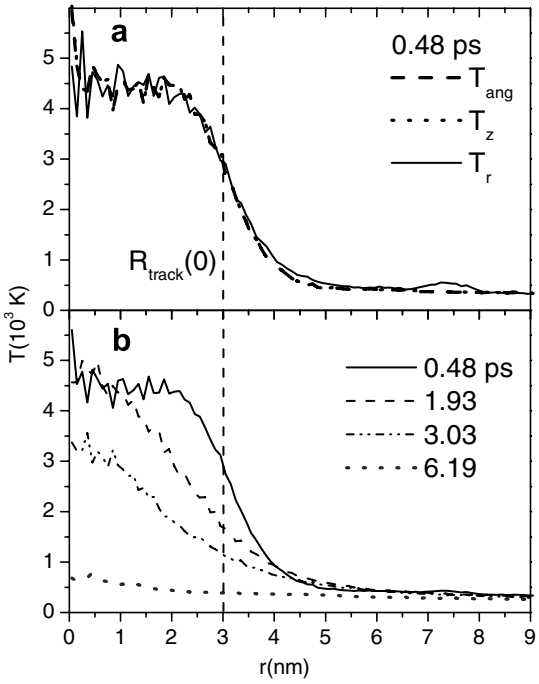

Fig. 3. Ion track in diamond, 50% efficiency (large sample): (a) temperature profiles at 0.48 ps, showing local thermal equilibrium. The small "bump" in the temperature profile is due to the "radial" wave; (b) temperature profiles at different times, showing the persistence of the hot track even at 1.93 ps.

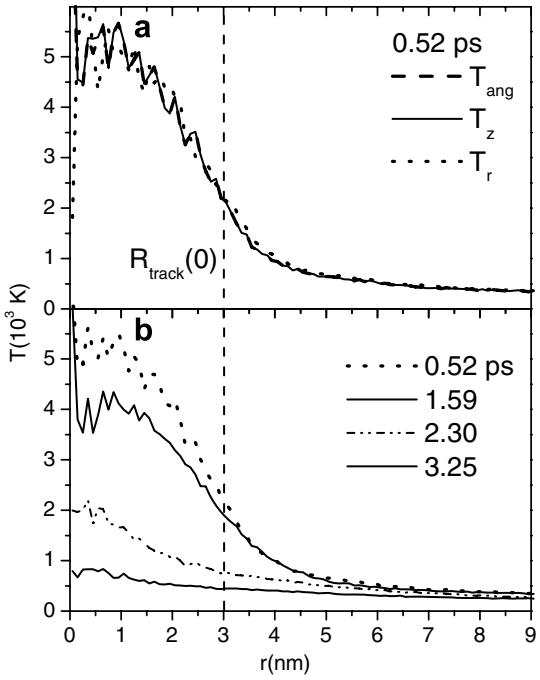

Fig. 4. Ion track in graphite, 50% efficiency (large sample): (a) temperature profiles at 0.52 ps, showing local thermal equilibrium. The shock wave already left the region shown in the figure; (b) temperature profiles at different times, showing the persistence of the hot track even at 1.59 ps.

results of [21,26], where cooling was assumed to occur over a time scale of ~0.3 ps. Even if the sample is allowed to cool down to near the original temperature, the final defect density and distribution might change significantly at long times beyond the scope of MD simulations. Kinetic Monte Carlo [54] or temperature accelerated dynamics (TAD) [55] simulations might be used to study this long time defect evolution, which might lead to re-crystallization. Our values for the amorphization threshold are therefore, only an upper estimate.

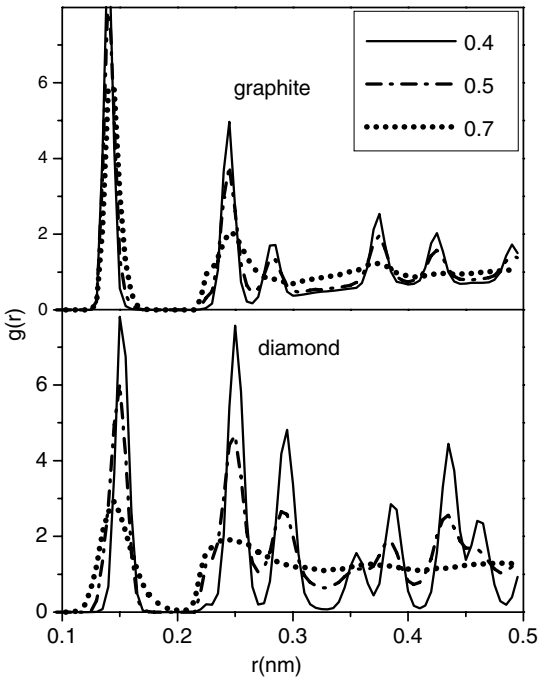

Fig. 5. Pair correlation function for both diamond and graphite at different excitation efficiencies.

In order to confirm the amorphous state of the tracks we calculate the pair correlation function, $g(r)$, in a cylinder of 1 nm radius around the track center. Replacement of the peaks beyond the second nearest neighbor shell in $g(r)$ by a roughly horizontal line at $g(r) = 1$ indicates the lack of long range order, which is the signature of the amorphous state. Results are shown in Fig. 5 and they confirm the qualitative observation from Fig. 1, i.e. tracks amorphizes for efficiencies of 70% or larger.

4. Summary and discussion

Our studies show that large-scale thermal spike simulations in diamond and graphite do produce tracks that are amorphous during at least several ps after irradiation if the efficiency in the transfer of energy from the electrons to the lattice is ~70% or more, i.e. the effective dE/dx has to be at least 6 ± 0.9 keV/nm for graphite and 10.5 ± 1.5 keV/nm for diamond for any experimental value of dE/dx. Damage tracks have generally not been seen in experiments of diamond anvil cell irradiation up to energy losses of 44 keV/nm [4,5], indicating that the electron–phonon coupling must be inefficient for diamond or that exciton diffusion is very rapid. For graphite, on the other hand, Liu et al. [8] found out that an experimental dE/dx of 7.3 ± 1.5 keV/nm was needed to create electronic damage in graphite when nuclear effects were factored out. We note that an efficiency of 0.5 (effective $dE/dx \sim 4.4$ keV/nm) already produces significant damage. Comparing the effective dE/dx needed to produce damage to the experimental dE/dx [7] implies a large efficiency for graphite.

Although the electron–phonon coupling 'constant', g, can be estimated from ab initio calculations or semi-analytical models [31,32], it has been pointed out that this coupling could be greatly different under non-equilibrium conditions [34]. Our simulated thresholds can help providing bounds to g under such conditions. For graphite $g \sim 3 \pm 10^{13}$ W/cm^3/K was obtained by fitting to the ion-beam damage threshold [13]. This is approximately the same value as g for amorphous carbon [13]. Given that amorphous materials typically have high values of g, this supports our statement above about the high efficiency for graphite.

Different track radii and excitation energies need to be explored to fully understand the track evolution and the connection to experimental results, but our initial simulation results are already consistent with experiments.

Studies of the coordination of the atoms inside and close to the track are in progress. This would allow for a direct comparison with spectroscopic measurements of irradiated samples which measure sp^2/sp^3 coordination changes. In addition, simulated TEM images of defect structures from

our simulations would also provide a direct comparison with experimental results. Future simulations of samples with a surface might also display the "bumps" seen in AFM studies of irradiated carbon materials [1,2]. Comparison of the size of these bumps between experiments and simulations would provide further constrains to the electron–phonon coupling efficiency.

Acknowledgments

The work was performed under the auspices of the US Department of Energy by University of California, Lawrence Livermore National Laboratory under contract of No. W-7405-Eng-48, with support from the Laboratory Directed Research and Development program. M. Toulemonde, A. Dunlop, G. Rizza, G. Schwietz and C. Trautmann provided valuable comments. We would like to thank M.J. Caturla and A. Kubota for sharing their parallel Brenner potential routines, and W. van Breugel and the Computational Materials Science Summer School at LLNL for their support. D.S. thanks for support from the German BMBF under Grant No. 05 KK4MGA/9.

References

[1] L.P. Biró et al., Nucl. Instr. and Meth. B 148 (1999) 1102.
[2] V.S. Varichenko et al., Diamond Relat. Mater. 3 (1994) 711.
[3] D.S. Misra et al., Thin Solid Films 503 (2006) 121.
[4] L.P. Biró, J. Gyulai, K. Havancsak, Nucl. Instr. and Meth. B 122 (1997) 476.
[5] M. Lang et al., Appl. Phys. A 80 (2005) 691.
[6] U.A. Glasmacher, M. Lang, H. Keppler et al., Phys. Rev. Lett. 96 (2006) 195701.
[7] A. Dunlop, private communication.
[8] J. Liu et al., Phys. Rev. B 64 (2001) 184115.
[9] M. Waiblinger et al., Appl. Phys. A: Mater. 69 (1999) 239.
[10] N. Koenigsfeld et al., Diamond Relat. Mater. 12 (2002) 469.
[11] D. Schwen, C. Ronning, H. Hofsäss, Diamond Relat. Mater. 13 (2004) 1032.
[12] G. Schiwietz et al., Europhys. Lett. 47 (3) (1999) 384.
[13] M. Caron, H. Rothard, M. Toulemonde, B. Gervais, M. Beuve, Nucl. Instr. and Meth. B 245 (2006) 36.
[14] R. Smith, Proc. R. Soc. London, Ser. A 431 (1990) 143.
[15] R. Smith, K. Beardmore, Thin Solid Films 272 (1996) 255.
[16] M. Kerford, R.P. Webb, Nucl. Instr. and Meth. B 153 (1999) 270.
[17] K. Nordlund, J. Keinonen, T. Mattila, Phys. Rev. Lett. 77 (1996) 699.
[18] E. Salonen et al., Phys. Rev. B 63 (2001) 195415.
[19] J. Marian et al., Phys. Scripta T 124 (2006) 65.
[20] D. Saada, J. Adler, R. Kalish, Phys. Rev. B 59 (1999) 6650.
[21] N.A. Marks, N.C. Cooper, D.R. McKenzie, D.G. McCulloch, P. Bath, S.P. Russo, Phys. Rev. B 65 (2002) 075411.
[22] N.A. Marks, Phys. Rev. B 56 (1997) 2441.
[23] J. Tersoff, Phys. Rev. Lett. 61 (1988) 2879.
[24] D.W. Brenner, Phys. Rev. B 42 (1990) 9458 (Corrigendum, Phys. Rev. B 46 (1992) 1948).
[25] S.J. Stuart et al., J. Chem. Phys. 112 (2000) 6472.
[26] A. Sorkin, J. Adler, R. Kalish, Phys. Rev. B 70 (2004) 064110.
[27] R.L. Fleischer, P.B. Price, R.M. Walker, Nuclear Tracks in Solids, Univ. California Press, Berkeley, 1975.
[28] G.H. Vineyard, Radiat. Eff. 29 (1976) 245.
[29] E. Johnson, R. Evatt, Radiat. Eff. 52 (1980) 187.
[30] P. Sigmund, C. Claussen, J. Appl. Phys. 52 (1981) 990.
[31] G. Szenes, Nucl. Instr. and Meth. B 122 (1997) 530.
[32] Z.G. Wang, C. Dufour, E. Paumier, M. Toulemonde, J. Phys.: Condens. Matter 6 (1994) 6733.
[33] M. Toulemonde et al., Phys. Rev. Lett. 88 (2002) 057602.
[34] A.E. Volkov, V.A. Borodin, Nucl. Instr. and Meth. B 193 (2002) 381.
[35] H.M. Urbassek, H. Kafemann, R.E. Johnson, Phys. Rev. B 49 (1994) 786.
[36] E.M. Bringa, R.E. Johnson, M. Jakas, Phys. Rev. B 60 (1999) 15107.
[37] M. Jakas, E.M. Bringa, R.E. Johnson, Phys. Rev. B 65 (2002) 165425.
[38] M. Beuve et al., Phys. Rev. B 68 (2003) 125423.
[39] O.J. Tucker et al., Nucl. Instr. and Meth. B 228 (2005) 163.
[40] E.M. Bringa, R.E. Johnson, Phys. Rev. Lett. 88 (2002) 165501.
[41] P. Durham et al., Astrophysical Letters, submitted for publication.
[42] R. Devanatham, R. Corrales, Nucl. Instr. and Meth. B, submitted for publication.
[43] T. Diaz de la Rubia, M.W. Guinan, Mat. Res. Forum 174 (1990) 151. http://www.llnl.gov/asci/platforms/purple/rfp/benchmarks/limited/mdcask/.
[44] H.U. Jäger, K. Albe, J. Appl. Phys. 88 (2000) 1129.
[45] J.N. Glosli, F.H. Ree, J. Appl. Phys. 110 (1999) 441.
[46] A.C.T. van Duin, private communication.
[47] J.F. Ziegler, J.P. Biersack, U. Littmark, The Stopping and Range of Ions in Solids, Pergamon Press, New York, 1985.
[48] R.E. Johnson, J. Schou, Mat. Fys. Medd. Dan. Vid. 43 (1993) 403.
[49] T.A. Tombrello, Nucl. Instr. and Meth. B 94 (1994) 424.
[50] E.M. Bringa, R. Papaleo, R.E. Johnson, Phys. Rev. B 65 (2002) 094113.
[51] H.O. Jeschke, M.E. Garcia, K.H. Bennemann, Phys. Rev. Lett. 87 (2001) 015003.
[52] M. Moseler, J. Nordiek, H. Haberland, Phys. Rev. B 56 (1997) 15439.
[53] J.K. Krüger et al., Diamond Relat. Mater. 9 (2000) 123.
[54] D. Landau, K. Binder, A Guide to Monte Carlo Simulations in Statistical Physics, Cambridge University Press, Cambridge, 2000.
[55] B. Uberaga et al., Phys. Rev. Lett. 92 (2004) 115505.